Monatshefte für Chemie 137, 583–593 (2006)
DOI 10.1007/s00706-006-0444-x

Monatshefte für Chemie
Chemical Monthly
Printed in Austria

Metal Oxoclusters as Molecular Building Blocks for the Development of Nanostructured Inorganic–Organic Hybrid Thin Films#

Silvia Gross[1,*], **Andrea Zattin**[2], **Vito Di Noto**[2], and **Sandra Lavina**[2]

[1] CNR–ISTM, Department of Chemistry, University of Padova and INSTM, I-35131 Padova, Italy
[2] Department of Chemistry, University of Padova, Padova, Italy

Received December 6, 2005; accepted (revised) January 16, 2006
Published online March 10, 2006

Summary. Silica-based inorganic–organic hybrid thin films embedding the organically modified oxohafnium clusters ($Hf_4O_2(OMc)_{12}$, OMc=OC(O)–C(CH_3)=CH_2) were obtained by photo-activated free radical copolymerisation of the methacrylate groups of the cluster with those of the pre-hydrolysed (methacryloxypropyl)trimethoxysilane (*MAPTMS*, (CH_2=C(CH_3)C(O)O)$(CH_2)_3Si(OCH_3)_3$). By this route, a covalent anchoring of the cluster to the forming silica network was achieved. Samples characterized by two different Si/Hf compositions (18:1, 5:1) were prepared. The surface and in-depth composition of the thin films were investigated through *Fourier* transform infrared spectroscopy (FT-IR) and X-ray photoelectron spectroscopy (XPS). XPS depth profiles performed on the thin layers evidenced a homogenous in depth distribution of the hafnium guest species within the whole silica films and sharp film-substrate interfaces.

Broad band dielectric spectroscopy (BDS) measurements permitted to investigate the electric response of the obtained films in the frequency and temperature range of 40 Hz – 1 MHz and 0–160°C.

Keywords. Methacryloxytrialkoxysilanes; Inorganic–organic hybrid materials; Thin films; Broad band dielectric spectroscopy.

Introduction

Inorganic–organic materials are currently a widely explored field of research since they enable the integration and the combination of useful organic and inorganic characteristics within a single molecular scale composite. The synthesis approaches to these materials and their manifold current and future applications

* Corresponding author. E-mail: silvia.gross@unipd.it
# Dedicated to *Ulrich Schubert* for his 60th birthday

have been throughly described in several papers and in some comprehensive recent reviews [1–13]. As highlighted by *Mitzi* [14], many potential applications of hybrid materials rely on the availability of easy and reliable thin film deposition methods. The possibility to cast inorganic–organic materials into films discloses further new applicative perspectives in several fields ranging from tribological materials [15], to solid-state solar cells [16], to the development of luminescent [17, 18], nonlinear optical [19], photonic [20], and microelectronic devices [21, 22]. The embedding of nanosized inorganic building blocks into polymeric films has been shown to result in improved mechanical [23–26], adhesion [27], optical [28, 29], and electric [30] properties. Hybrid thin films have also been used as precursors for nanoporous low-*k* dielectrics [31] and they have been extensively used for the development of protective coatings as reported by *Sanchez et al.* [1]. Recent developments and state of the art on inorganic–organic hybrid thin films have been reported and throughly discussed by *Mitzi* in an extensive review [14] as well as in the earlier mentioned review article [1]. One of the most used approaches to process hybrid thin layers is the sol–gel method, which can be described as the formation of an oxide network by the progressive hydrolysis and polycondensation reactions of a sol, a stable suspension of colloidal particles of a suitable molecular precursor in a liquid medium, to give a gel, a porous three-dimensional continuous solid network surrounding a liquid phase [32]. Sol–gel can be extended to the preparation of hybrid layers by using metal alkoxides functionalised with organic groups. Suitable functionalisation of the alkoxides with organic groups enables the implementation of the sol–gel process for the development of an inorganic network embedding organic parts. In this framework, a plethora of ORMOCER® (organic modified ceramic) and ORMOSIL (organic modified silicate) have been designed, patented, and commercialized by the *Fraunhofer* Institut für Silikatforschung [1, 9], which are based on the introduction of organic groups into an inorganic framework by using organoalkoxysilane molecular precursors $R'_n - \mathrm{Si}(\mathrm{O}R)_{4-n}$. Inorganic–organic hybrid thin films have been prepared based on glycidoalkyltrialkoxysilanes [17], methacryloxysilanes [25], polymethylsilsesquioxanes [21, 31], acrylic resin-silica [33, 34], silica-polyurethane nanocomposites [24, 35], and polysilane-methacrylate copolymers [29, 36]. Further examples of inorganic–organic hybrid thin films concern polyimide-silica hybrids [37, 38]. We have recently optimised a procedure to prepare silica-based inorganic–organic hybrid materials which, upon calcination at high temperature, convert into mixed oxides. The homogeneous distribution of the cluster in the hybrid silica matrix is retained upon annealing, thus yielding metal oxide guest nanoparticles evenly embedded in the silica network. By using this procedure, both thin film and powders have been prepared [39–43]. In this study, the methacrylate-substituted transition metal oxocluster $\mathrm{Hf_4O_2(O}Mc)_{12}$ and the methacryloxypropyltrimethoxysilane were used to prepare silica-based hybrid thin films embedding hafnium oxoclusters, as sketched in Scheme 1.

This cluster was synthesised by reaction of hafnium butoxide with methacrylic acid as reported elsewhere [45]. These and similar metal oxoclusters have been already used as inorganic building blocks for the synthesis of a wide variety of inorganic–organic hybrid materials [2–13]. In our approach a chemical grafting of the two components is ensured by photo-activated polymerisation of the methacrylates, while the alkoxy groups of the silane undergo hydrolysis and condensa-

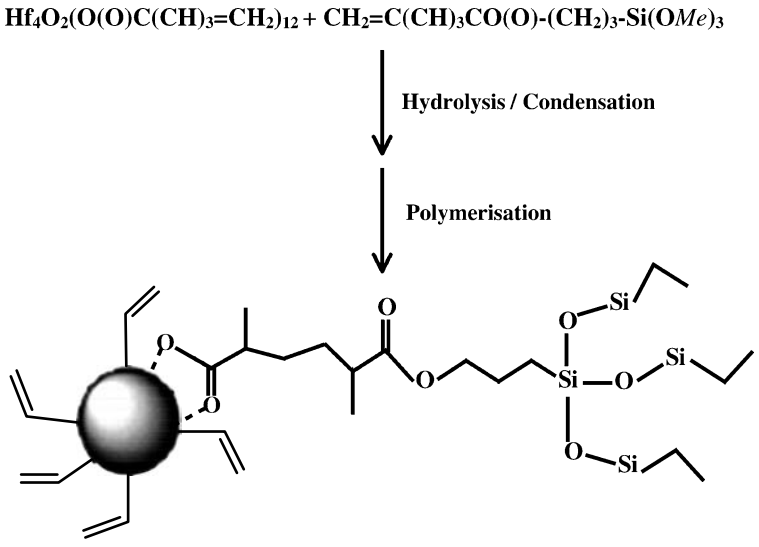

Scheme 1. Scheme for the radical polymerisation between the silane and the hafnium cluster

tion reactions to form a silica network. The silane has to be pre-hydrolysed before polymerisation takes place, since otherwise the "frozen" polymeric structure would suppress the mobility required for the condensation of the alkoxy groups. Once prepared, the hybrid materials were throughly investigated. In particular, the surface composition and the in-depth distribution of the host hafnium oxocluster in the silica matrix were analysed by performing XPS depth profiles, whereas the electric properties of the materials were revealed carrying out detailed analyses on complex permittivity spectra of film materials.

Results and Discussions

IR spectroscopy was used to investigate the composition of the thin films containing the hafnium clusters in different amounts. In Fig. 1 the IR spectra of the samples SiHf5 (a), SiHf18 (b) and Si (c) are compared. The detected peaks were assigned according to the values reported [46–51], and the main vibrational bands are evidenced and labelled in the graphs. IR spectra show that, already in the hybrid films, the formation of a polysiloxane network is evident. In particular, the typical vibrations of silica are well evident in all the samples as the typical band of the silica network at about $780\,cm^{-1}$ was detected, which is ascribed to the symmetric stretching of oxygen in the Si–O–Si group [49]. Furthermore, the intense band at $1110\,cm^{-1}$, ascribed to the ν_{as}(Si–O–Si) antisymmetric stretching of the siloxane group, and the band at $470\,cm^{-1}$, ascribed to the rocking vibrations of the Si–O–Si, were also detected [52, 53]. In addition, all the vibrations typical of the organic components of the matrix could be detected: the peaks at 2890 and $2950\,cm^{-1}$, ascribed to the $\nu_{as}(CH_3)$ antisymmetric stretching of methyl groups and to the ν_s(CH) symmetric stretching of the terminal methylene double bonds [52]. Well evident are also the sharp band at $1720\,cm^{-1}$ for ν(C=O) and the less

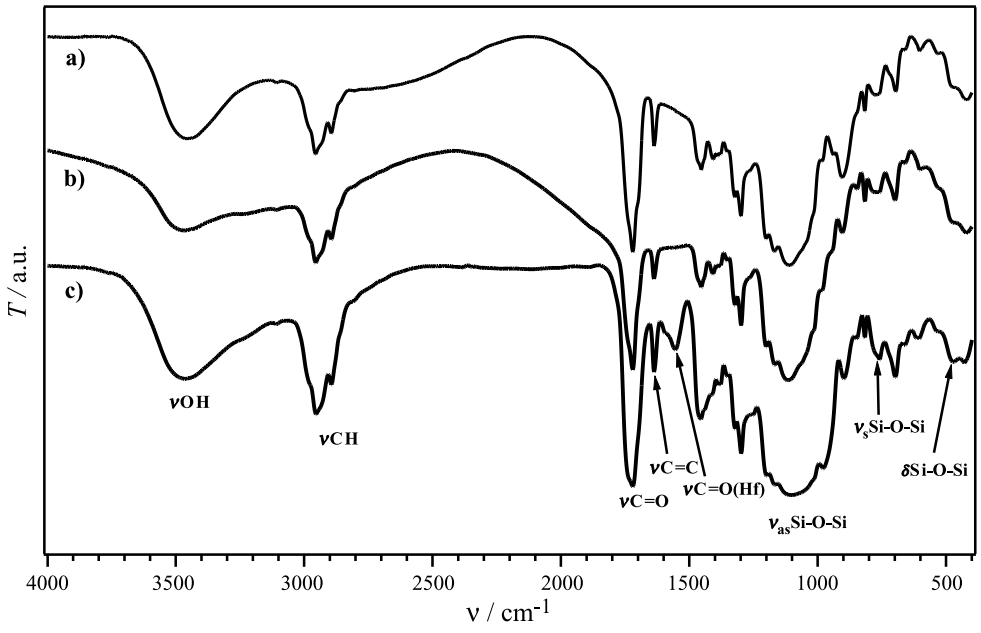

Fig. 1. Superimposed FT-IR spectra of the samples a) Si, b) SiHf18, and c) SiHf5

intense but still present band at about 1635 cm^{-1} attributed to the unreacted C=C of the methacrylate moieties. In the most concentrated sample, a further band at 1556 cm^{-1} was evidenced, which was ascribed, accordingly to further studies [54], to the vibration of the chelating carboxylate groups of the methacrylate moieties of the cluster. These features should disappear upon complete polymerisation. However, due to the hampered mobility of the methacrylate groups, which are covalently linked to the already partially formed silica network and also to the steric restrictions imposed by the cluster bearing 12 methacrylate groups, a complete copolymerisation of the cluster methacrylate groups with the methacryloxysilane could not be achieved. The amount of double bonds still present can be related to the extent of the polymerisation of the materials. The degree of crosslinking achieved by the UV photoinduced polymerisation process was monitored by FT-IR. Since the absolute intensity of the IR bands cannot be compared, the ratio between two bands was taken into account, namely the C=C and the C=O bonds. As the polymerisation process proceeds, the intensity of the acrylate ν(C=C) band at about 1635 cm^{-1} decreases due to the C=C double bonds consumption, while the integrated area of the ν(C=O) bands remains constant. Consequently, the ν(C=O)/ν(C=C) area ratio was considered as a measure of the degree of conversion. By using this method, the following scale for the degree of crosslinking in the three different materials could be determined: SiHf18 > Si > SiHf5. These data can be interpreted by considering that the cluster acts as crosslinking point, since it is surrounded by 12 units from which polymerisation can depart. However, a high amount of cluster is expected to lead to statistically less favoured polymerisation.

XPS measurements were used to achieve information on the surface and in-depth composition of the thin films. For comparison, the surface XPS spectrum of

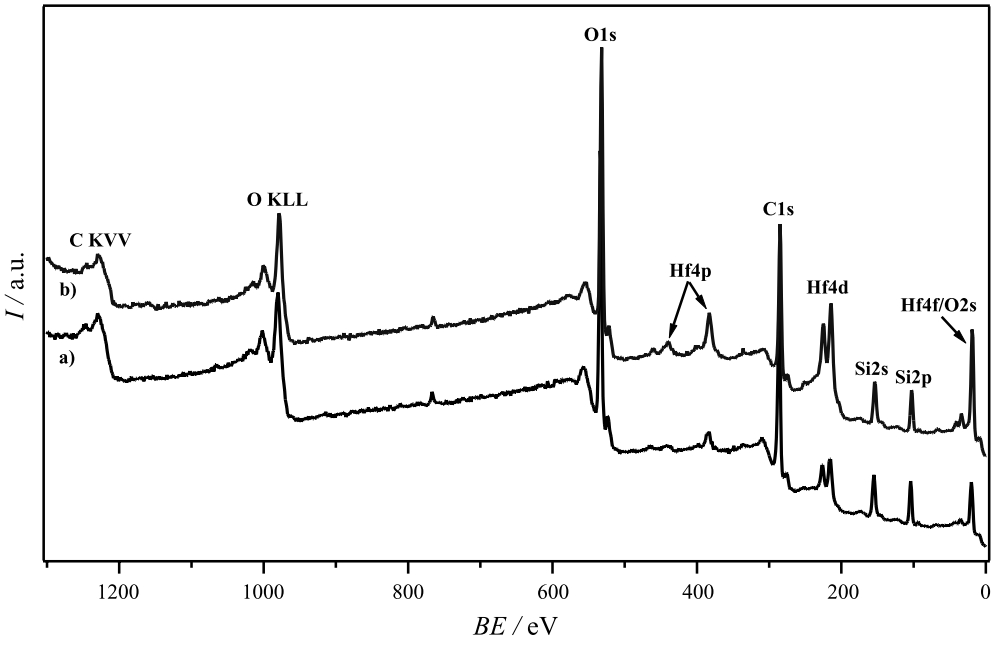

Fig. 2. Superimposed XPS surveys of a) SiHf18 and b) SiHf5

the UV polymerised *MAPTMS* (Si) as-prepared was also acquired. In Fig. 2, the survey spectra of samples SiHf5 and SiHf18 are superimposed. In the oxocluster-containing samples the hafnium peaks (Hf4f, Hf4d, and Hf4p) are well evident, as well as the peaks of all the other elements (C, Si, and O).

The in-depth composition of the films was analysed by performing depth profiles. By plotting the ratio of the atomic percentages *vs.* time of sputtering, which

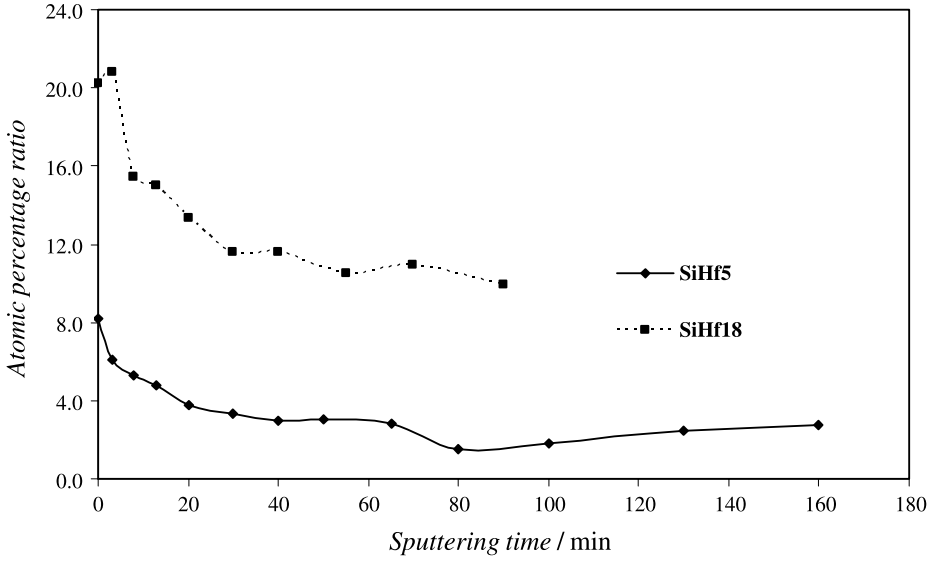

Fig. 3. XPS profiles of the samples SiHf5 and SiHf18 as function of time of sputtering

can be in turn related to the eroded depth, it can be seen that the guest species, the hafnium clusters, are quite evenly distributed along the whole film thickness. The in-depth XPS profiles of the samples SiHf5 and SiHf18 are shown in Fig. 3.

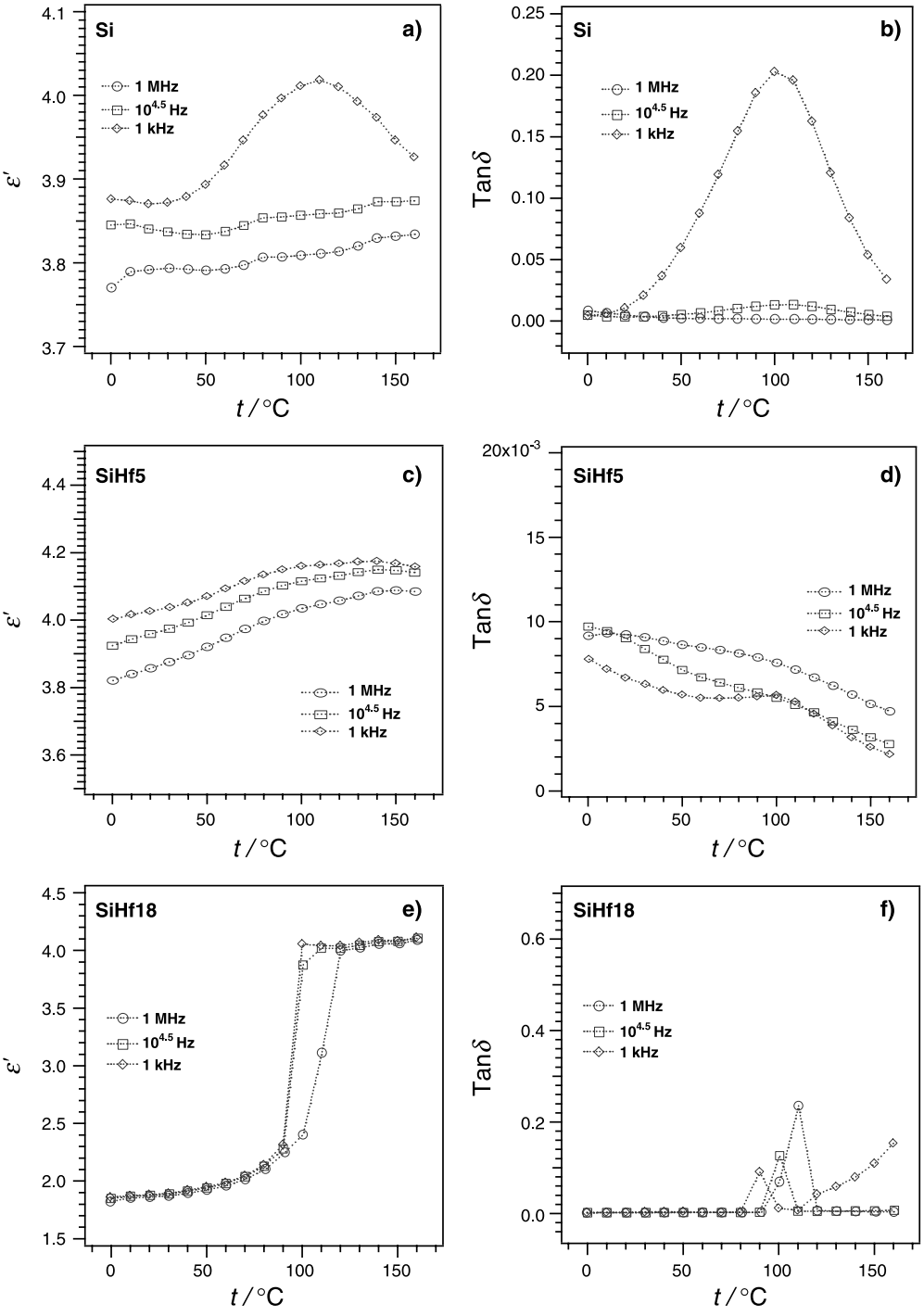

Fig. 4. Temperature dependence spectra of the real permittivity, $\varepsilon'(\omega)$ (a, c, e) and tanδ (b, d, f) profiles of Si, SiHf5, and SiHf18 samples

In the samples SiHf5 and SiHf18, the Si/Hf atomic ratio obtained by XPS is about 3 and 15. These data are in agreement with the theoretical ones, *i.e.* 5 and 18.

The electric response of the hybrid films Si, SiHf18, and SiHf5 was investigated by broad band dielectric spectroscopy in the frequency and temperature range 40 Hz – 1 MHz and 0–160°C. Figures 4a, 4c, and 4e show the temperature spectra of the real component of permittivity measured at 1 kHz, 32 kHz, and 1 MHz. A detailed analysis of the ε' temperature spectra profiles reveals that the permittivity of the measured films varies in the range 3.75–4.05 ($\Delta\varepsilon' = 0.3$), 3.8–4.2 ($\Delta\varepsilon' = 0.4$), and 1.8–4.3 ($\Delta\varepsilon' = 2.5$) for materials Si, SiHf5, and SiHf18. These results indicate that the effect of the Hf cluster on the dielectric dispersion of the material is much more evident in the sample with lowest concentration ($\Delta\varepsilon' = 2.5$). This latter sample exhibits the lowest value of dielectric permittivity ($\varepsilon' = 1.8$). These results could be explained if we consider the effect of dipolar contribution of silicon and Hf cluster moieties to the total cumulative dipole moments of the systems expressed in terms of overall polarization of the materials. Particularly, the comparison of the cluster sample concentrations and $\Delta\varepsilon'$ values indicates that the samples Si and SiHf5 behave in a similar way, thus indicating that a) the transition registered in the spectra of ε' at *ca.* 100°C corresponds to the same crosslinking event associated to the silicon based monomer; b) the polarization behavior and the degree of dipole moment reorganization is similar in both materials. These conclusions are in agreement with IR data which show that for the two samples a very similar crosslinking density is revealed as evaluated from the C=O/C=C intensity ratios. This information indicates that a high cluster concentration in the hybrid materials probably induces a phase segregation between cluster and silicon based polymer chains which thus generates materials with similar relaxation events. On the other hand the sample SiHf18 presents a different profile of ε' vs. temperature, Fig. 5a, and permittivity values lower than 2 below 70°C. These indications demonstrate that when the reaction is carried out at low cluster concentrations, the cluster moiety is efficiently crosslinked with silicon monomers thus producing a hybrid inorganic–organic network were Hf clusters are bonded together through silicon based chains. This phenomenon generates voids in bulk materials which lower the permittivity of the obtained films.

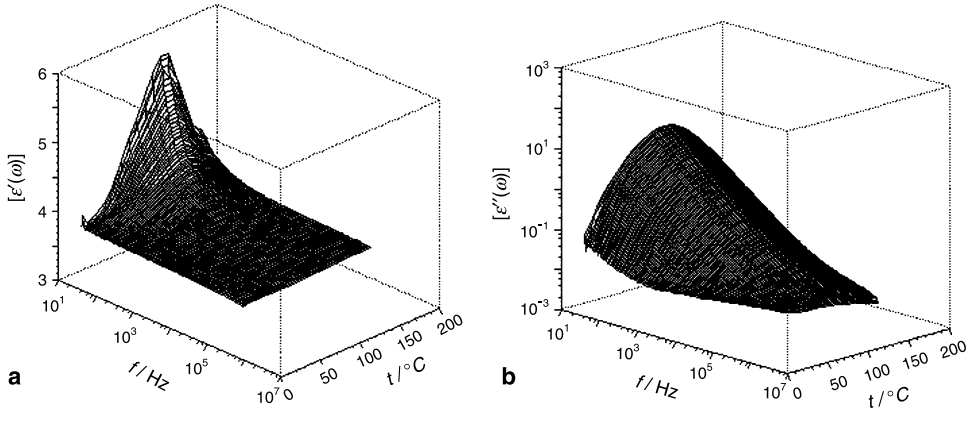

Fig. 5. Real (a), $\varepsilon'(\omega)$, and imaginary (b), $\varepsilon''(\omega)$, components of the dielectric permittivity of a Si film

The dependence on temperature of dielectric tanδ of the investigated films are reported in Figs. 4b, 4d, and 4f. These curves confirm the above described results, showing a similar thermal relaxation event at high frequency for Si and SiHf5. This phenomenon seems to be absent in the sample SiHf18; in this case, the low amount of Hf clusters is completely embedded in polymer backbone. In addition, for sample SiHf18 below 70°C tanδ values are below 0.05. All these results suggest that SiHf18 seems to be an interesting material to be used as insulator gate film in microelectronic devices such as field effect transistors.

In conclusion, the analysis of temperature dielectric spectra allows to conclude that the effect of void generated by the large Hf clusters is more efficient when the concentration of these ones is low. On the other hand a high oxocluster concentration gives rise to a phase segregation in products with physical properties such as those of a composite material obtained by treating a polymer with an inorganic filler. As an example, the Figs. 5a and 5b show the real and imaginary components of permittivity spectra of a Si sample. In these plots are revealed the relaxation event above described centered at 100°C with a contribution of σ_{DC} conduction. The σ_{DC} charge transfer events are revealed in the steep increase of the ε'' profiles as the frequency decreases.

The presence of this effect is revealed significantly in Si and SiHf5 samples, whereas in SiHf18 a weak contribution of σ_{DC} is detected. These results confirm the above hypotheses that at 100°C a) in Si and SiHf5 the crosslinking reaction of samples is competed with molecular relaxations and charge transfer phenomena; and b) molecular relaxations and host medium reorganizations occur mainly at 100°C.

Conclusions

In conclusion, the proposed synthesis protocol seems to be promising for the preparation of materials to be used as dielectric films for the development of gates in field effect transistors operating at temperatures lower than 70°C. Particularly interesting is sample SiHf18, which in the measured temperature and frequency range exhibits a permittivity slightly lower than 2 and a tan$\delta < 0.05$.

Experimental

Methacryloxypropyltrimethoxysilane (*MAPTMS*) and Hf(O*Bu*)$_4$ purchased from ABCR, Karlsruhe, Germany; anhydrous *THF*, anhydrous toluene, and methacrylic acid 99% were purchased from Aldrich. The photoinitiator Irgacure 184 was a gift by Ciba Specialty Chemicals, Basel, Switzerland. The cluster $Hf_4O_2(OMc)_{12}$ was synthesised by the previously reported procedure [45].

Precursors Solutions

All handlings were performed under Ar using standard *Schlenk* techniques. The preparation of the starting solution used for the film deposition is a three-step process, which is schematically sketched in Fig. 6. Experimental details are reported in Refs. [39, 40]. Different solutions characterised by different Si/Hf molar ratios were prepared; labels "SiHf number" indicate the specimens prepared by using the Hf oxocluster while the number indicates the Si/Hf atomic ratio. The label "Si" indicates the sample without clusters used as a reference.

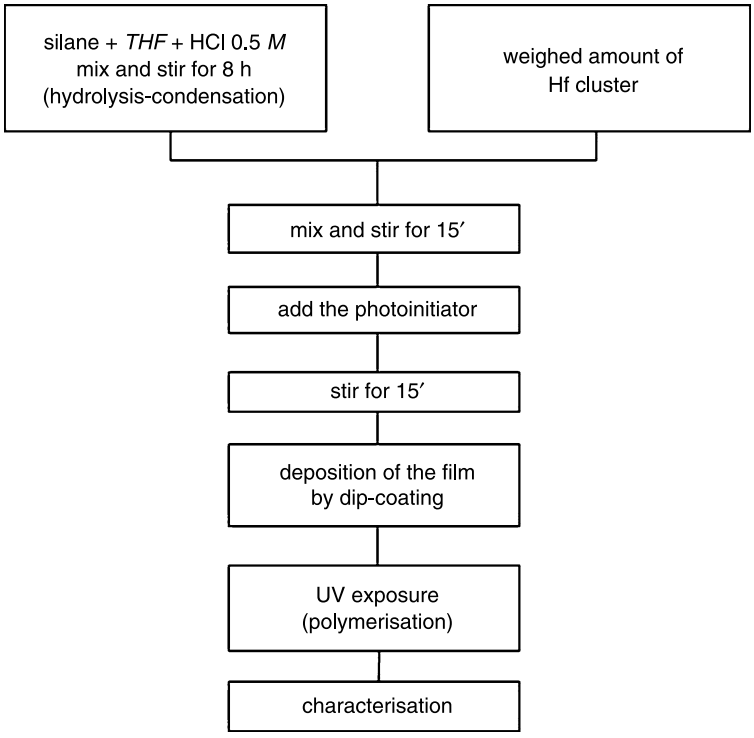

Fig. 6. Flow chart of the synthesis procedure

Film Deposition and UV Curing

The films were prepared *via* a dip-coating procedure using a home-made equipment. The dip-coating film deposition was carried out in air at a constant withdrawal speed of 10 cm min^{-1} (room temperature, relative humidity 30–40%). Four different materials were used as Si wafers (Si 110), soda-lime slides, Herasil silica slides, supplied by Hereaus and K-glass slides (EKOPLUS, 11×8 mm, 3 mm thick, consisting of glass one-side coated with a thin film of fluorine doped tin oxide, supplied by Isoclima (Este, PD, Italy)). After dip-coating, the films were irradiated with a Helios Italquartz s.r.l. lamp, 125 W for 10 min to promote the polymerisation of the metharylate moieties of the cluster and of the silane. The irradiation time was optimised on the basis of time-dependent IR measurements [40]. Homogeneous, transparent, smooth, and well adherent films were obtained on all the substrates.

Thin Films Characterization

FT-IR spectra were recorded in transmission with a Nexus 870 FT-IR spectrometer (Nicolet) from 400 to 4000 cm^{-1}, resolution 4 cm^{-1}. The films for the analyses were spun onto a one side polished Si wafer. The composition of the film at the surface and in the bulk was investigated by XPS. These spectra were run on a Perkin-Elmer Φ 5600 ci spectrometer using non-monochromatized Al–K_α radiation (1486.6 eV). The atomic composition was evaluated using sensitivity factors [55]. Depth profiles were carried out by Ar^+ sputtering at 2 kV with an Ar partial pressure of 5×10^{-6} Pa. The measurements of complex permittivity spectra were carried out in the frequency range 40 Hz – 11 MHz using three types of equipment: a laboratory-made dielectric spectrometer consisting of a charge amplifier and a digital data acquisition system in the range 10 mHz – 100 kHz; and a Hewlett-Packard HP4192ALF in the range 5 Hz – 13 MHz. The measurements were performed on films deposited on a 20 mm in diameter circular stainless steel electrode. The thickness of the films was determined by using a micrometer. The samples were placed in a cryostat whose temperature was controlled by a N_2

gas jet heating and cooling system operating from 0 to +160°C. The complex permittivity, $\varepsilon^*(\omega) = \varepsilon'(\omega) - i\varepsilon''(\omega)$ was measured, where $\omega = 2\pi f$ (f = frequency in Hz).

Acknowledgements

Ministero degli Affari Esteri, Rome, Italy and Österreichischer Austauschdienst (ÖAD), Vienna, Austria are gratefully acknowledged for the funding of the researchers mobility in the framework of an Haly-Austria bilateral program. *S. Gross* gratefully thanks the Deutscher Akademischer Austauschdienst (DAAD), Bonn, Germany, for the awarding of a DAAD grant. Ciba Specialty Chemicals, Basel, Schweiz, is acknowledged for the kind supply of Irgacure 184. *S. G.* is very indebted to *U. Schubert* for his teachings of science, life, and for teaching her that "Am Ende kommt immer die Belohnung".

References

[1] Sanchez C, Julian B, Belleville P, Popall M (2005) J Mater Chem **15**: 3559, and references therein
[2] Chem Mater, Special Issue on Organic-Inorganic Nanocomposite (2001) **13**(10)
[3] Sanchez C, Soler-Illia GJdAA, Ribot F, Lalot T, Mayer CR, Cabuil V (2001) Chem Mater **13**: 3061
[4] Sanchez C, Ribot F, Lebeau B (1999) J Mat Chem **9**: 35
[5] Sanchez C, Ribot F (1993) J Physique **3**: 1349
[6] Wen J, Wilkes GL (1996) Chem Mater **8**: 1667
[7] Sharp KG (1998) Adv Mater **10**: 1243
[8] Loy DA (2001) MRS Bulletin 364
[9] Spanhel L, Popall M, Müller G (1995) Proc Ind Acad Sci: Chem Sci **107**: 637
[10] Schubert U (2001) Chem Mat **13**: 3487, and references therein
[11] Kickelbick G (2003) Prog Polym Sci **28**: 83
[12] Schubert U (2003) J Sol-Gel Sci Techn **26**: 47
[13] Schubert U (2003) Polymers Reinforced by Covalently-Bonded Metal Oxide Clusters, in: Organic/Inorganic Hybrid Materials, Electronic Publ. Services: Hattiesburg)
[14] Mitzi DB (2001) Chem Mater **13**: 3283
[15] Qi CZ, Gao H, Yan FY, Liu WM, Bao GQ, Sun XD, Chen JM, Zheng XM (2005) J Appl Poly Sci **97**: 38
[16] Robertson LB, Poggi MA, Kowalik J, Smestad GP, Bottomley LA, Tolbert LM (2004) Coord Chem Rev **248**: 1491
[17] Que WX, Hu X (2005) Surface Coat Techn **198**: 40
[18] Li YH, Zhang HJ, Wang SB, Meng QG, Li HR, Chuai XH (2001) Thin Solid Films **385**: 205
[19] Lee KS, Kim TD, Min Yh, Yoon CS, Samoc M, Samoc A (2000) Mol Cryst Liqu Cryst **353**: 525
[20] Seddom AB (1998) Iee Proc Circ Dev Syst **145**: 369
[21] Yang CC, Wu PT, Chen WC, Chen HL (2004) Polymer **45**: 5691
[22] Houbertz J, Schulz J, Froelich L, Domann G, Popall M (2003) Mater Res Soc Symp: 769
[23] Atanacio AJ, Latella BA, Barbe CJ, Swain MV (2005) Surf Coat Techn **192**: 354
[24] Chen YC, Zhou SX, Yang HH (2005) J Appl Polym Sci **95**: 1032
[25] Xiong MN, Zhou S, Wu L, Wang B, Yang L (2004) Polymer **45**: 8127
[26] Que WX, Hu X (2003) J Vac Sci Techn A **21**: 1809
[27] Chou TP, Cao GZ (2003) J Sol-Gel Sci Techn **27**: 31
[28] Yu YY, Chen CY, Chen WC (2003) Polymer **44**: 593
[29] Mimura S, Naito H, Kanemitsu Y, Matsukawa H (2000) J Organomet Chem **611**: 40
[30] Kagan CR, Mitzi DB, Dimitrakopoulos CD (1999) Science **286**: 945

[31] Lazzeri P, Vanzetti L, Anderle M, Bersani M, Park JJ, Lin Z, Briber R, Rubloff G, Kim HC, Miller RD (2005) J Vac Sci Techn B **23**: 908
[32] Schubert U, Hüsing N (2000) Synthesis of Inorganic Materials, Wiley-VCH, Weinheim
[33] Xiong MN, Zhou SX, You B, Gu GX, Wu LM (2004) J Polym Sci B-Polymer Phys **42**: 3682
[34] Xiong MN, You B, Zhou SX, Wu LM (2004) Polymer **45**: 2967
[35] Chen YC, Zhou SX, Yang HH, Gu GX, Wu LM (2004) J Coll Interf Sci **279**: 370
[36] Matsukawa K, Fukui S, Higashi N, Niwa M, Inoue H (1999) Chem Lett **10**: 1073
[37] Chang CC, Wei KH, Chen WC (2003) J Electrochem Soc **150**: F147
[38] Ha CS, Cho WJ (1999) Macromol Symp **142**: 205
[39] Armelao L, Bleiner D, Di Noto V, Gross S, Sada C, Schubert U, Tondello E, Vonmont H, Zattin A (2005) Appl Surf Sci **249**: 277
[40] Armelao L, Eisenmenger-Sittner C, Groenewolt M, Gross S, Sada C, Schubert U, Tondello E, Zattin A (2005) J Mater Chem **15**: 1838
[41] Armelao L, Bertagnolli H, Gross S, Krishnan V, Lavrencic-Stangar U, Müller K, Orel B, Srinivasan G, Tondello E, Zattin A (2005) J Mater Chem **15**: 1954
[42] Armelao L, Gross S, Tondello E, Zattin A (2005) Surf Sci Spectra **10**: 157
[43] Armelao L, Gross S, Tondello E, Zattin A (2005) Surf Sci Spectra **10**: 150
[44] Armelao L, Barreca D, Bottaro G, Gasparotto A, Gross S, Maragno C, Tondello E, Zattin A (2005) Surf Sci Spectra **10**: 137
[45] Gross S, Kickelbick G, Puchberger M, Schubert U (2003) Monatsh Chem **134**: 1053
[46] Neumayer DA, Cartier E (2001) J Appl Phys **90**: 1801
[47] Del Monte F, Larsen W, Mackenzie JD (2000) J Am Cer Soc **83**: 628
[48] Nishide T, Honda S, Matsuura M, Ide M (2000) Thin Solid Film **371**: 61
[49] Innocenzi P (2003) J Non-Cryst Solids **319**: 309
[50] Bertoluzza A, Fagnano C, Morelli MA, Gottardi V, Guglielmi M (1982) J Non-Cryst Solids **48**: 117
[51] Parler CM, Ritter JA, Amiridis M (2001) J Non-Cryst Solids **279**: 119
[52] Saravanamuttu K, Xin Min D, Najafi SI, Andrews MP (1998) Can J Chem **76**: 1717
[53] Zhan Z, Zeng HC (1999) J Non-Cryst Solids **243**: 26
[54] Armelao L, Gross S, Müller K, Pace G, Tondello E, Tsetsgee O, Zattin A, in preparation
[55] Moulder F, Stickle WF, Sobol PE, Bomben KD (1991) Handbook of X-Ray Photoelectron Spectroscopy, Perkin Elemer Corporation, Eden Prairie MN